

# Non-Fickian diffusion and tau-approximation from numerical turbulence

Axel Brandenburg\*

NORDITA, Blegdamsvej 17, DK-2100 Copenhagen Ø, Denmark

Petri Käpylä†

Kiepenheuer-Institut für Sonnenphysik, Schöneckstraße 6, D-79104 Freiburg, Germany and

Department of Physical Sciences, Astronomy Division,  
P.O. Box 3000, FIN-90014 University of Oulu, Finland

Amjad Mohammed‡

Physics Department, Oldenburg University, 26111 Oldenburg, Germany

(Dated: May 22, 2019, Revision: 1.38 )

Evidence for non-Fickian diffusion of a passive scalar is presented using direct simulations of homogeneous isotropic turbulence. The results compare favorably with an explicitly time-dependent closure model based on the tau-approximation. In the numerical experiments three different cases are considered: (i) zero mean concentration with finite initial concentration flux, (ii) an initial hat profile for the concentration, and (iii) an imposed background concentration gradient. All cases agree in the resulting relaxation time in the tau-approximation relating the triple correlation to the concentration flux. The first order smoothing approximation is shown to be inapplicable.

PACS numbers: 52.65.Kj, 47.11.+j, 47.27.Ak, 47.65.+a

## I. INTRODUCTION

In a turbulent flow the transport of a passive scalar is an important problem in atmospheric research, astrophysics, and combustion [1, 2]. Passive scalar transport is also an important benchmark for more complicated turbulent transport processes such as turbulent magnetic diffusion and the alpha-effect in dynamo theory [3, 4], or turbulent viscosity and its non-diffusive counterparts such as the AKA-effect [5, 6] and the Lambda effect [7, 8].

Modeling turbulent transport in terms of turbulent diffusion is known to have major deficiencies. For example turbulent transport is known to be anomalous, i.e. the width  $\sigma$  of a localized patch of passive scalar concentration may expand in time like  $\sigma^2 \sim t^\beta$ , where  $\beta = 1$  corresponds to ordinary (Brownian) diffusion,  $\beta > 0$  is superdiffusion, and  $\beta < 0$  is subdiffusion [9]. Thermal convection, for example, has superdiffusive properties [12]. Turbulent transport is also known to have nonlocal and non-diffusive properties. One of the outcomes of this realization was the development of the transients matrix approach [10, 11] which captures nonlocal transport properties, although only in a diagnostic fashion [12]. In order to describe nonlocal aspects in a prognostic fashion, higher order spatial derivatives of the turbulent fluxes need to be included. These are best incorporated in terms of an integral kernel [13]. In the present work, however, instead of invoking higher order spatial derivatives, we follow the recent proposal of Blackman and Field [14, 15]

to include an additional second order *time derivative* instead. This turns the diffusion equation into a damped wave equation. In passive scalar transport theory this is sometimes referred to as non-Fickian diffusion [16, 17], where the second order time derivative is usually obtained by taking the zeroth and first moments of the one-dimensional Kramers equation.

Non-Fickian diffusion has also been discussed in various engineering applications. For example diffusion problems in a composite media [17, 18] and neutron transport problems in reactors [19] are best modeled using non-Fickian diffusion.

The reason the extra time derivative appears in the approach of Blackman and Field is that they start with calculating the time derivative of the passive scalar flux which then turns out to have a component proportional to the negative concentration gradient. This by itself leads to a wave equation. However, there is an important contribution from the triple corrections which are assumed to be proportional to the double correlation terms divided by some damping time (tau-approximation). This turns the equation into a *damped* wave equation. Blackman and Field argued that wave-like behavior is unphysical, but, as it will turn out, the simulations presented below give evidence for mildly wave-like behavior in certain parameter regimes. It is important to emphasize that the classical first order smoothing approximation [4, 20] breaks down because it assumes that the triple correlations are simply negligible. In fact, it turns out that the triple correlations are as important as the quadratic correlations.

Adding an extra time derivative in the way mentioned above does certainly solve another long standing problem. Solutions to the diffusion equation are known to violate causality, because the diffusion equation is ellip-

\*Electronic address: brandenb@nordita.dk

†Electronic address: petri.kapyla@oulu.fi

‡Electronic address: amjad@mail.uni-oldenburg.de

tic and the propagation speed of a signal is infinite [21]. This problem was originally discussed in the context of general relativity [22], and more recently in the context of black hole accretion [23, 24]. The extra time derivative affects the modeling of turbulent transport most strongly at early times, just after having injected the passive scalar. This additional time derivative term tends to make the turbulent transport more ballistic at early times (corresponding to  $\beta \approx 2$ ). This is actually a well known property also of standard Brownian motion.

The objective of the present paper is twofold. First we need to find out whether the existence of the proposed additional time derivative can actually be confirmed using turbulence simulations. If so, we need to find out the magnitude of this extra term. Second, we need to study the range of modifications expected from this new term. In order to do this we consider numerical simulations of weakly compressible turbulence including the transport of a passive scalar.

We begin by discussing the formalism that leads to the emergence of the additional time derivative in mean field theory. We then discuss the type of simulations carried out and present three numerical experiments that quantify the relative importance of the additional time derivative and that support the tau-approximation formalism.

## II. FIRST ORDER SMOOTHING VERSUS $\tau$ -APPROXIMATION

A classic application of passive scalar transport is the diffusion of smoke in a turbulent atmosphere. If the smoke is injected in one point it will diffuse radially outward, so the mean concentration is expected to be a function of radius  $r$  and time  $t$ . In that case it makes sense to consider averages over spherical shells, i.e.

$$\overline{C}(r, t) \equiv \frac{1}{4\pi} \int_0^{2\pi} \int_0^\pi C(r, \theta, \phi, t) \sin \theta \, d\theta \, d\phi, \quad (1)$$

where  $C$  is the concentration per unit volume. Another application is the passive scalar diffusion between two parts of a slab that is initially separated by a membrane. In that case the mean concentration varies along the direction of the slab, say  $z$ , and then it makes sense to define horizontal averages, i.e.

$$\overline{C}(z, t) \equiv \frac{1}{L_x L_y} \int_0^{L_x} \int_0^{L_y} C(x, y, z, t) \, dx \, dy. \quad (2)$$

This is also the type of average that is best suited for studies in cartesian geometry considered here.

For clarity of the presentation we ignore here microscopic diffusion, in which case  $C$  satisfies the simple conservation equation,

$$\frac{\partial C}{\partial t} = -\nabla \cdot (\mathbf{U}C), \quad (3)$$

where  $\mathbf{U}$  is the fluid velocity. The effects of finite microscopic diffusion will be discussed in the appendix. We now split  $\mathbf{U}$  and  $C$  into mean and fluctuating parts, i.e.

$$\mathbf{U} = \overline{\mathbf{U}} + \mathbf{u}, \quad C = \overline{C} + c, \quad (4)$$

and average Eq. (3), so we have

$$\frac{\partial \overline{C}}{\partial t} = -\nabla \cdot (\overline{\mathbf{U}} \overline{C} + \overline{\mathbf{u}c}). \quad (5)$$

The challenge is now to find an expression for the concentration flux,  $\overline{\mathbf{u}c} \equiv \overline{\mathcal{F}}$  in terms of the mean concentration,  $\overline{C}$ . The standard approach is to express the departure of the concentration from its average,  $c \equiv C - \overline{C}$ , in terms of its past evolution, i.e.

$$c(\mathbf{x}, t) = \int_0^t \dot{c}(\mathbf{x}, t') \, dt', \quad (6)$$

where the dot denotes time differentiation and

$$\dot{c} \equiv \dot{C} - \dot{\overline{C}} = -\nabla \cdot (\overline{\mathbf{U}}c + \mathbf{u}\overline{C} + \mathbf{u}c - \overline{\mathbf{u}c}) \quad (7)$$

is the evolution equation for the passive scalar fluctuation obtained by subtracting Eq. (5) from (3). In the first order smoothing approximation or, which is the same, the second order correlation approximation [7], one *ignores* the terms that are nonlinear in the fluctuations, i.e.  $\mathbf{u}c - \overline{\mathbf{u}c}$  in Eq. (7) are simply omitted [3, 4]. This is only justified if microscopic diffusion is large (but we have already neglected it) or if the velocity is delta-correlated in time, which is also unrealistic.

By contrast, in the  $\tau$ -approximation [25] the quadratic term  $\mathbf{u}c$  is not ignored. This term leads to a triple correlation,  $\overline{u_i u_j \partial_j c}$ , which is then approximated by a relaxation term proportional to the quadratic correlation  $\mathbf{u}c$ . This is reminiscent of the Eddy-Damped Quasi-Normal Markovian approximation [25, 26, 27], where fourth order correlations are approximated by third order correlations. Recently, Blackman and Field [15] applied a similar idea to magnetohydrodynamics and to the present problem of passive scalar transport. They proposed to calculate not  $\overline{\mathcal{F}}$ , but instead its time derivative. In that case the time integration in Eq. (7) disappears and one has

$$\frac{\partial \overline{\mathcal{F}}}{\partial t} = \overline{\mathbf{u}(\mathbf{x}, t) \dot{c}(\mathbf{x}, t)} + \overline{\dot{\mathbf{u}}(\mathbf{x}, t) c(\mathbf{x}, t)}. \quad (8)$$

This leads to the final equation

$$\frac{\partial \overline{\mathcal{F}}_i}{\partial t} = -\overline{u_i u_j} \partial_j \overline{C} - \frac{\overline{\mathcal{F}}_i}{\tau}, \quad (9)$$

where  $\tau$  is some relaxation time and incompressibility has been assumed, i.e.  $\partial_j u_j = 0$ . We shall now also assume isotropy,  $\overline{u_i u_j} = \frac{1}{3} \delta_{ij} u_{\text{rms}}^2$ , where  $u_{\text{rms}}$  is the rms velocity with  $u_{\text{rms}}^2 = \overline{\mathbf{u}^2}$ . The validity of Eq. (9) is clearly something that ought to be checked numerically using turbulence simulations. This is the main objective of the present paper.

The other aspect is that the time derivative may not be ignorable in the final set of evolution equations. Thus, in contrast to ordinary Fickian diffusion, where the passive scalar flux  $\bar{\mathcal{F}}$  is assumed to be proportional to the mean negative concentration gradient (Fick's law), i.e.

$$\bar{\mathcal{F}} = -\kappa_t \nabla \bar{C} \quad (\text{Fickian diffusion}), \quad (10)$$

where  $\kappa_t = \frac{1}{3}\tau_{\text{cor}} u_{\text{rms}}^2$  is the turbulent passive scalar diffusivity and  $\tau_{\text{cor}}$  is some correlation time, one has now [15]

$$\bar{\mathcal{F}} = -\kappa_t \nabla \bar{C} - \tau \frac{\partial \bar{\mathcal{F}}}{\partial t} \quad (\text{non-Fickian}), \quad (11)$$

where  $\kappa_t = \frac{1}{3}\tau u_{\text{rms}}^2$ . Equation (10) can be reconciled only when time variations of the concentration flux have become small and if the correlation time  $\tau_{\text{cor}}$  is identified with the damping time  $\tau$ .

Applying  $\partial_t + \tau^{-1}$  on both sides of (5), ignoring for simplicity a mean flow ( $\bar{\mathbf{U}} = 0$ ), and inserting (11) yields a damped wave equation,

$$\frac{\partial^2 \bar{C}}{\partial t^2} + \frac{1}{\tau} \frac{\partial \bar{C}}{\partial t} = \frac{1}{3} u_{\text{rms}}^2 \nabla^2 \bar{C}. \quad (12)$$

We note in passing that the extra term is in some ways analogous to the displacement current in the Maxwell equations. This is why this equation is also known in the literature as the Cattaneo–Maxwell equation [28]. The maximum signal speed is limited by  $u_{\text{rms}}/\sqrt{3}$ . Assessing the importance of the extra time derivative is another objective of the present paper.

The only ill-known free parameter in this theory is  $\tau$ , whose value is conveniently expressed in terms of the Strouhal number [4],

$$\text{St} = \tau u_{\text{rms}} k_f, \quad (13)$$

where  $k_f$  is the forcing wavenumber or, more generally, the wavenumber of the scale of the energy carrying eddies.

Some preliminary estimate of St can be made by considering the late time behavior where Fickian diffusion holds. From Eq. (10) we expect that the decay rate of a large scale pattern with wavenumber  $k_1$  is

$$\lambda_c = \kappa_t k_1^2, \quad (14)$$

where  $\kappa_t = \frac{1}{3}\tau u_{\text{rms}}^2$  is the turbulent diffusion coefficient. From forced turbulence simulations with initial mean flow or mean magnetic field patterns [29], the decay rates of these patterns are well described by a turbulent kinematic viscosity,  $\nu_t$ , and a turbulent magnetic diffusion coefficient,  $\eta_t$ , where both coefficients are about equally large with

$$\nu_t \approx \eta_t \approx (0.8 \dots 0.9) \times u_{\text{rms}}/k_f. \quad (15)$$

Applying the same value also to  $\kappa_t$  we obtain

$$\text{St} \approx (0.8 \dots 0.9) \times 3 = 2.4 \dots 2.7. \quad (16)$$

This result is remarkable in view of the fact that in the classic first order smoothing approach to turbulent transport coefficients one has to assume  $\text{St} \ll 1$ ; see Refs [4, 20].

### III. COMPARISON WITH SIMULATIONS

In order to test the viability of the non-Fickian diffusion approach and to determine the value of St we have designed three different types of turbulence simulations. We first consider the problem of a finite initial flux,  $\bar{\mathcal{F}}$ , but with zero mean concentration,  $\bar{C} = 0$  [15]. Next we consider the evolution of an initial hat profile for  $C$  and finally we investigate the case of an imposed uniform gradient of  $C$  which leads to the most direct determination of  $\tau$  as a function of Reynolds number and forcing wavenumber. We begin with a brief description of the simulations carried out.

#### A. Summary of the type of simulations

We consider subsonic turbulence in an isothermal gas with constant sound speed  $c_s$  in a periodic box of size  $2\pi \times 2\pi \times 2\pi$ . The Navier-Stokes equation for the velocity  $\mathbf{U}$  is written in the form

$$\frac{D\mathbf{U}}{Dt} = -c_s^2 \nabla \ln \rho + \mathbf{F}_{\text{visc}} + \mathbf{f}, \quad (17)$$

where  $D/Dt = \partial/\partial t + \mathbf{U} \cdot \nabla$  is the advective derivative,

$$\mathbf{F}_{\text{visc}} = \nu (\nabla^2 \mathbf{U} + \frac{1}{3} \nabla \nabla \cdot \mathbf{U} + 2\mathbf{S} \cdot \nabla \ln \rho) \quad (18)$$

is the viscous force where  $\nu = \text{const}$  is the kinematic viscosity,  $\mathbf{S}_{ij} = \frac{1}{2}(U_{i,j} + U_{j,i}) - \frac{1}{3}\delta_{ij}U_{k,k}$  is the traceless rate of strain tensor, and  $\mathbf{f}$  is a random forcing function (see below). The continuity equation is

$$\frac{\partial \rho}{\partial t} = -\nabla \cdot (\mathbf{U} \rho), \quad (19)$$

and the equation for the passive scalar concentration per unit volume,  $C$ , is

$$\frac{\partial C}{\partial t} = -\nabla \cdot \left[ \mathbf{U} C - \rho \kappa_C \nabla \left( \frac{C}{\rho} \right) \right], \quad (20)$$

where  $\kappa_C = \text{const}$  is the diffusion coefficient for the passive scalar concentration, which is related to  $\nu$  by the Schmidt number,

$$\text{Sc} = \nu/\kappa_C. \quad (21)$$

Throughout this work we take  $\text{Sc} = 1$ . A nondimensional measure of  $\nu$  and hence  $\kappa_C$  is the Reynolds number, which is here defined with respect to the inverse forcing wavenumber,

$$\text{Re} = u_{\text{rms}} / (\nu k_f). \quad (22)$$

The maximum possible value of  $\text{Re}$  depends on the resolution and the value of  $k_f$ . For  $k_f = 1.5$  the typical value is approximately equal to the number of meshpoints in one direction.

We adopt a forcing function  $\mathbf{f}$  of the form

$$\mathbf{f}(\mathbf{x}, t) = \text{Re}\{N \mathbf{f}_{\mathbf{k}(t)} \exp[i\mathbf{k}(t) \cdot \mathbf{x} + i\phi(t)]\}, \quad (23)$$

where  $\mathbf{x} = (x, y, z)$  is the position vector, and  $-\pi < \phi(t) < \pi$  is a ( $\delta$ -correlated) random phase. The normalization factor is  $N = f_0 c_s (k c_s / \delta t)^{1/2}$ , with  $f_0$  a nondimensional forcing amplitude,  $k = |\mathbf{k}|$ , and  $\delta t$  the length of the timestep; we chose  $f_0 = 0.05$  so that the maximum Mach number stays below about 0.5 (the rms Mach number is close to 0.2 in all runs.) The vector amplitude  $\mathbf{f}_{\mathbf{k}}$  describes nonhelical transversal waves with  $|\mathbf{f}_{\mathbf{k}}|^2 = 1$  and

$$\mathbf{f}_{\mathbf{k}} = (\mathbf{k} \times \mathbf{e}) / \sqrt{\mathbf{k}^2 - (\mathbf{k} \cdot \mathbf{e})^2}, \quad (24)$$

where  $\mathbf{e}$  is an arbitrary unit vector. At each timestep we select randomly one of many possible wave vectors in a finite range around the forcing wavenumber  $k_f$  (see below).

The equations are solved using the same method as in Ref. [30], but here we employ a new cache and memory efficient code [31] using MPI (Message Passing Interface) library calls for communication between processors. This allows us to run at a resolutions up to  $1024^3$  meshpoints [32, 33].

## B. Finite initial flux experiment

We consider first the example discussed by Blackman and Field [15]. In Fickian diffusion, if  $\bar{C} = 0$ , there should be no flux, i.e.  $\bar{\mathcal{F}} = 0$ . Although this should in general be correct, one can imagine contrived situations where this is not the case, so it is an ideal problem to test whether the inclusion of the extra time derivative of the flux is at all correct and meaningful. Without this extra time derivative  $\bar{C}$  would always stay zero.

To explain in simple terms what happens, consider a situation where we have initially uniformly mixed white and black balls (so  $\bar{C} = 0$ ), but for some reason the balls are given an initial push such that the white balls move to the right part of the domain and all the black balls move to the left part of the domain. Then, after a short time, there should be a systematic segregation of white and black balls, in spite of continuous random forcing. Of course, this segregation survives only for a dynamical time, after which ordinary diffusion will begin to mix white and black balls.

In order to set up such a situation in a turbulence simulation we assume that at  $t = 0$  the turbulence has already fully developed and then we initialize the passive scalar distribution according to

$$C(x, y, z, 0) = C_0 \frac{u_z(x, y, z, 0)}{u_{\text{rms}}} \sin k_1 z. \quad (25)$$

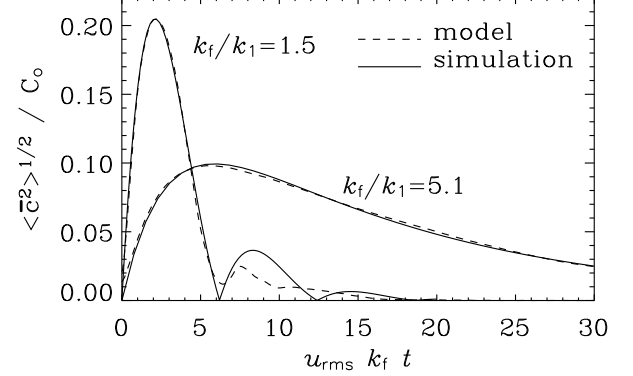


FIG. 1: Passive scalar amplitude,  $\langle \bar{C}^2 \rangle^{1/2} / C_0$ , versus time (normalized by  $u_{\text{rms}} k_f$ ) for two different values of  $k_f/k_1$ . The simulations have  $256^3$  meshpoints. The results are compared with solutions to the non-Fickian diffusion model.

Since  $\bar{u}_z = 0$ , and since the Reynolds rules [4] are obeyed by our horizontal averages, we have  $\bar{C}(z, 0) = 0$ , but because  $\bar{u}_z^2 \neq 0$ , we have  $\bar{\mathcal{F}}_z = \bar{u}_z \bar{C} \neq 0$ .

Numerically, we monitor the evolution of  $\langle \bar{C}^2 \rangle^{1/2}$ , where angular brackets denote an average over  $z$ . This is to be compared with the analytic solution of the model equation (12). Assuming that  $\bar{C}(z, t)$  is proportional to  $\exp(i k_1 z + \lambda t)$ , the two eigenvalues are

$$\lambda_{\pm}(k_1) = -\lambda_0 \pm \Delta\lambda(k_1), \quad (26)$$

where

$$\lambda_0 = \frac{u_{\text{rms}} k_f}{2 \text{St}}, \quad \Delta\lambda(k_1) = \sqrt{\lambda_0^2 - \frac{1}{3} u_{\text{rms}}^2 k_1^2}. \quad (27)$$

The solution that satisfies  $\bar{C}(z, 0) = 0$  is

$$\langle \bar{C}^2 \rangle^{1/2} = A \exp(-\lambda_0 t) \sinh(\Delta\lambda t), \quad (28)$$

where  $A$  is an amplitude factor. Oscillatory solutions are possible ( $\Delta\lambda$  imaginary) either when  $\text{St}$  is large enough or, since  $\text{St}$  cannot be manipulated in a simulation, when  $k_f$  is small enough. According to Eq. (16) we can estimate

$$k_f/k_1 < 2 \text{St}/\sqrt{3} \approx 3 \quad (\text{oscillatory behavior}). \quad (29)$$

In the oscillatory case,  $\Delta\lambda$  is imaginary and so  $\langle \bar{C}^2 \rangle^{1/2}$  is proportional to  $e^{-\lambda_0 t} |\sin \omega t|$ , where  $\omega = \text{Im} \Delta\lambda$ .

Note that the solution depends only on the combination  $\text{St}/k_f$ , where  $k_f$  should be a known input parameter for a given simulation. However, in order to be able to fit the model to the simulation we have considered  $\text{St}$  and  $k_f$  as independent fit parameters and refer then to the quantity  $k_f^{(\text{fit})}$ . The results of our fits of the simulations to the models is shown in Fig. 1. The corresponding fit parameters are listed in Table I.

TABLE I: Summary of fit parameters for the finite initial flux experiment. In all cases, the measured value of  $u_{\text{rms}} = 0.23$  is used. Note that  $k_f^{(\text{fit})}$  is an independent fit parameter used instead of  $k_f$  to model the solution for a given value of  $k_f$ . The range of wavenumbers used in the forcing function is also given.

$k_f/k_1$	(range)	$k_f^{(\text{fit})}/k_1$	$\text{St}^{(\text{fit})}$	$A^{(\text{fit})}$
1.5	(1...2)	1.0	1.8	0.21
2.2	(2...3)	1.6	1.8	0.38
5.1	(4.5...5.5)	3.8	2.4	0.18

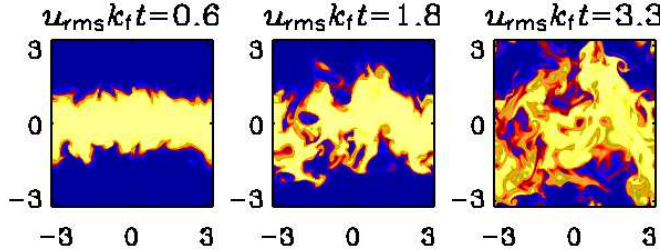


FIG. 2:  $C(x, 0, z)$  at three different times after reinitializing  $C$  according to Eq. (30).  $k_f/k_1 = 1.5$ ,  $\text{Re}_{\text{LS}} = 400$ .

We see that in all cases the Strouhal number does indeed exceed unity. The resulting value is close to the value based on our simple estimate in Eq. (16). Second, oscillatory behavior of the solution is not only mathematically possible for small values of  $k_f$ , see Eq. (26), but it is even physically realized in the solution for  $k_f/k_1 = 1.5$ .

#### IV. INITIAL HAT FUNCTION

Next we consider the problem of an initial step function. The advantage of such a profile as initial condition is that a broad spectrum of wavenumbers is excited. In order to avoid sharp jumps in the initial condition we choose a smoothed hat function using the initial profile

$$C(x, y, z, 0) = \frac{1}{2} + \frac{1}{2} \tanh[k_z^2(d^2 - z^2)], \quad (30)$$

where  $k_z = 2$  and  $d = 1$  throughout this work.

It is important to start the experiment at a time when the turbulence is fully developed. A visualization of  $C$  at three different times after reinitializing  $C$  is shown in Fig. 2.

For Fickian diffusion the initial hat function will broaden and develop eventually into a gaussian. As usual, for large enough values of the Strouhal number, wave-like behavior is possible and this would correspond to the initial bump splitting up into two bumps traveling in opposite directions. We have not been able to see this in our simulations so far. We have therefore decided to introduce as a quantitative measure of the departure

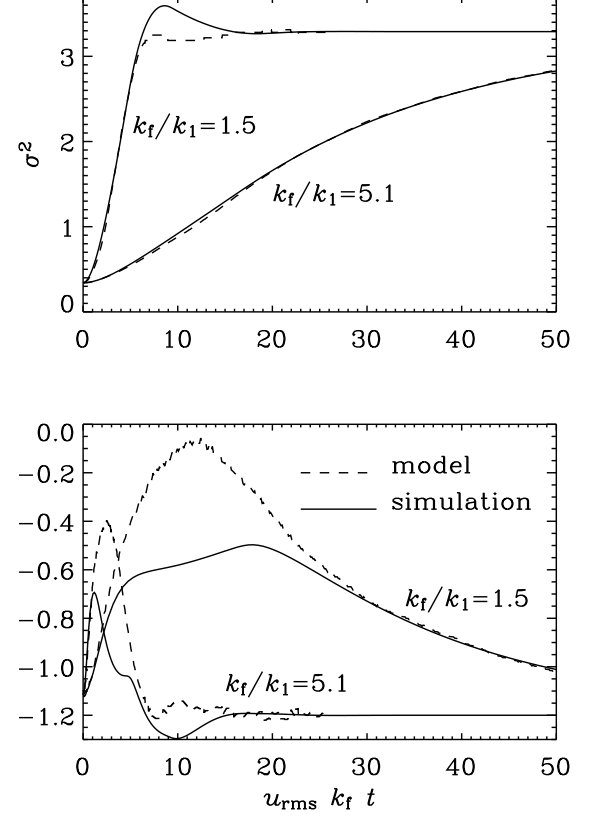


FIG. 3: Comparison of the evolution of  $\sigma^2$  and the kurtosis  $\kappa - 3$  for the non-Fickian diffusion model and the simulation. Note the good agreement at early and late times, but there are departures at intermediate times. The simulations have  $256^3$  meshpoints.

from a gaussian profile the kurtosis,

$$\kappa = \frac{1}{\sigma^4} \frac{\int C z^4 dz}{\int C dz}, \quad (31)$$

where  $\sigma$  quantifies the width of the profile with

$$\sigma^2 = \frac{\int C z^2 dz}{\int C dz}. \quad (32)$$

For a gaussian profile we have  $\kappa = 3$ , so we always plot  $\kappa - 3$ .

At early times,  $\sigma^2$  increases quadratically with  $t$ , but it approaches soon the linear regime,  $\sigma^2 \sim t$ , until  $\sigma$  saturates at a value comparable to the scale of the box; (12).

In Fig. 3 we compare the simulation results for  $\sigma^2$  and  $\kappa - 3$  with those obtained from the model (12) using the same boundary conditions (periodic in  $z$ ) and for the same values of  $u_{\text{rms}}$ . For simplicity we solve Eq. (12) numerically. However, similarly to the cases considered in the previous subsection, we are unable to obtain good fits if we choose exactly the same values of  $k_f$  as in the

TABLE II: Summary of fit parameters for the initial hat function experiment. In all cases, the measured value of  $u_{\text{rms}} = 0.23$  is used. Note that the values of  $\text{St}^{(\text{fit})}$  are the same as those used in the previous subsection, and the values of  $k_f^{(\text{fit})}$  are now slightly closer to  $k_f$  than before.

$k_f/k_1$	$k_f^{(\text{fit})}/k_1$	$\text{St}^{(\text{fit})}$
1.5	1.3	1.8
2.2	2.0	1.8
5.1	4.6	2.4

simulation. Therefore, like in the previous subsection, we treat  $k_f$  as a fit parameter denoted by  $k_f^{(\text{fit})}$ ; see Table II.

There are characteristic departures in the values of  $\sigma^2$  and  $\kappa - 3$  for the model compared with the simulations. This could perhaps be explained by the fact that, especially when  $k_f/k_1$  is of order unity, the horizontal averages  $\bar{C}$  obtained from the simulations are strongly ‘contaminated’ by a small number of large eddies. Nevertheless, both at early and at late times the agreement between model and simulation is excellent.

The results in this subsection confirm our finding of § III B that  $\text{St}$  is around 2 (or even larger). Again, this is large enough for oscillatory effects to appear when  $k_f/k_1$  is small.

## V. IMPOSED MEAN CONCENTRATION GRADIENT

Finally, we consider the case of a uniform gradient in the mean concentration. It is advantageous to split  $C$  into two contributions,

$$C(x, y, z, t) = \rho(x, y, z, t)Gz + c(x, y, z, t), \quad (33)$$

where  $G = \text{const}$  is the imposed mean gradient of the concentration per unit mass (not unit volume). Although  $C$  is now no longer periodic, this choice still preserves periodic boundary conditions for the departure  $c$  from the background profile  $\rho Gz$ . In terms of  $c$  we have then

$$\frac{\partial c}{\partial t} = -\nabla \cdot \left[ \mathbf{U}c - \rho \kappa_C \nabla \left( \frac{c}{\rho} \right) - \rho \kappa_C G \hat{\mathbf{z}} \right] - \rho U_z G, \quad (34)$$

where  $\hat{\mathbf{z}}$  is the unit vector in the  $z$  direction. The main advantage of this setup is the fact that we can now define mean fields by averaging over the entire volume. We denote such averages by angular brackets. Note that  $\langle \mathbf{U} \rangle = 0$ , so  $\mathbf{U} = \mathbf{u}$ . The mean passive scalar flux is then  $\langle uc \rangle$  and the triple correlation arising from  $\langle u_z c \rangle$  is

$$T_1 = \langle u_z \nabla \cdot (\mathbf{u}c) \rangle. \quad (35)$$

Furthermore, there are triple correlation terms arising from the  $\langle \dot{u}_z c \rangle$  term via the momentum equation. The  $\mathbf{u} \cdot \nabla \mathbf{u}$  term yields the triple correlation

$$T_2 = \langle (\mathbf{u}c) \cdot \nabla u_z \rangle, \quad (36)$$

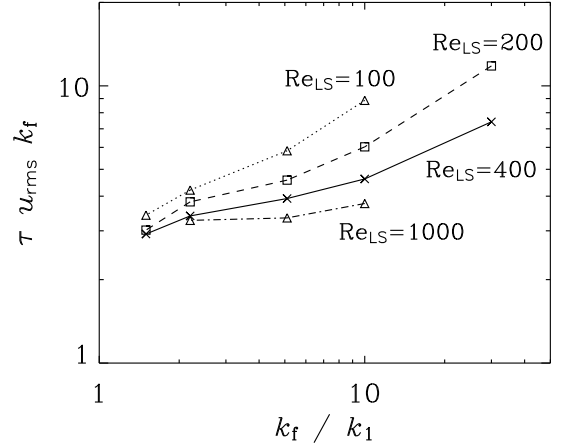


FIG. 4: Strouhal number as a function of  $k_f/k_1$  for different values of  $\text{Re}_{\text{LS}}$ . The resolution varies between  $64^3$  meshpoints ( $\text{Re}_{\text{LS}} = 100$ ) and  $512^3$  meshpoints ( $\text{Re}_{\text{LS}} = 1000$ ).

and the pressure gradient term,  $c_s^2 \nabla \ln \rho$ , yields

$$T_3 = \langle c \nabla_z h \rangle, \quad (37)$$

where  $h = c_s^2 \ln \rho$  is related to the enthalpy. There is no correlation arising from the forcing term, because the forcing is delta-correlated in time. Furthermore, the contributions from the viscous and diffusive terms are small. Because of periodic boundary conditions,  $T_1 + T_2 = 0$ , so the only contribution surviving from the sum of all three terms is  $T_3$ . Thus, the final expression for  $\tau$  is

$$\tau = \langle u_z c \rangle / \langle c \nabla_z h \rangle. \quad (38)$$

We note however, that on the average all contributions from the momentum equations balance, i.e.  $T_2 + T_3 = 0$ . Therefore it is also possible to calculate  $\tau$  from the contributions of the passive scalar equation alone, i.e.

$$\tau = \langle u_z c \rangle / \langle u_z \nabla \cdot (\mathbf{u}c) \rangle. \quad (39)$$

We have calculated a series of simulations for different values of the Reynolds number as a function of  $k_f$ . However, for a fixed values of  $\nu$ , since  $k_f$  changes, the Reynolds number, as defined by Eq. (22), is not constant. Therefore we label here the curve by the value of the large scale Reynolds number that we define as

$$\text{Re}_{\text{LS}} = u_{\text{rms}} / (\nu k_1). \quad (40)$$

The result is shown in Fig. 4.

The resulting value of  $\text{St}$  depends weakly on  $k_f$  and increases slowly with increasing  $k_f$ . This dependence is weaker for smaller values of  $k_f$ . As the Reynolds number increases, however, the range where  $\text{St}$  is approximately constant seems to increase. It is therefore conceivable

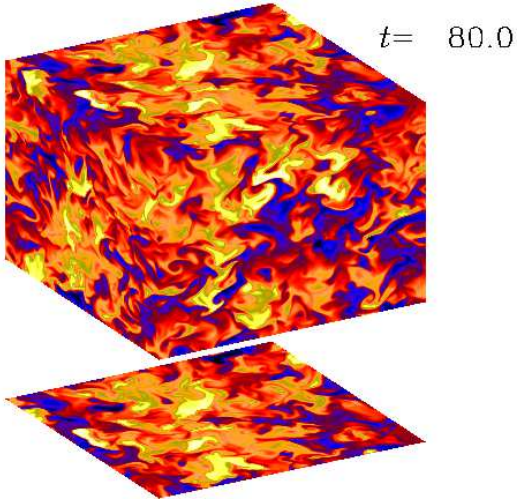


FIG. 5: Visualizations of  $C$  on the periphery of the simulation domain at a time when the simulation has reached a statistically steady state.  $k_f/k_1 = 5.1$ ,  $Re_{LS} = 400$ .

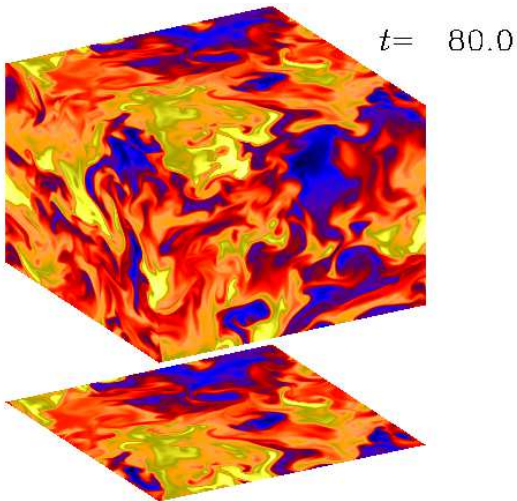


FIG. 6: Same as Fig. 5, but for  $k_f/k_1 = 1.5$ .

that  $St$  converges to a universal constant whose value is around 3.

Visualizations of  $C$  on the periphery of the simulation domain are shown in Figures 5 and 6 for  $k_f = 5.1$  and 1.5, respectively [34]. Note the combination of large patches (scale  $\sim 1/k_f$ ) together with thin filamentary structures. This is particularly clear in the case with  $k_f/k_1 = 1.5$ . The kinetic energy spectrum is close to  $k^{-5/3}$ , but the passive scalar spectrum is clearly shallower (perhaps like  $k^{1.4}$ ; see Fig. 7).

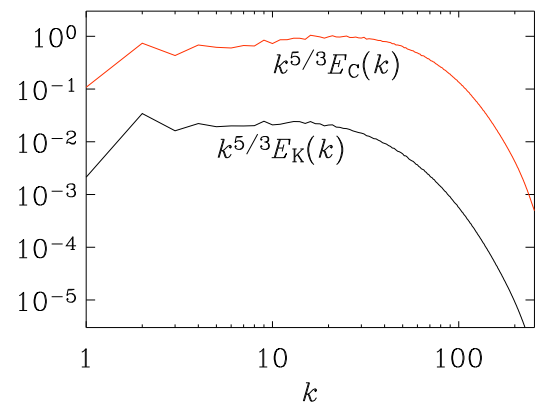


FIG. 7: Compensated kinetic energy and passive scalar spectra for the run with  $k_f/k_1 = 2.2$ ,  $Re_{LS} = 1000$ .

## VI. CONCLUSIONS

Two important results have emerged from the present investigation. First, the Strouhal number is generally above unity and may have a universal value between 2 and 3 for forced turbulence. This implies that the classical first order smoothing approach is invalid. Second, the triple correlations that are normally neglected are of comparable magnitude to the second order corrections that correspond to the passive scalar flux. The tau-approximation in which the two are assumed to be proportional to each other is shown to be justified.

As was shown recently by Blackman and Field in the context of magnetohydrodynamics [14] and then in the context of passive scalar diffusion [15], this leads to an additional time derivative in the mean field equation which then takes the form of a damped wave equation. Our work has now shown that when the forcing occurs on large enough scale ( $k_f \lesssim 2k_1$ ) there is evidence for mildly oscillatory behavior.

Among the various methods for determining the Strouhal number in a turbulence simulation, the approach of imposing a uniform gradient of the passive scalar concentration is the most direct one in that no fitting procedure is needed. Using this approach requires however a firm knowledge that the functional form of the mean field equation is correct. This underlines the importance of the first two approaches where we were able to compare the evolution of various statistical quantities with those obtained by solving the model equation. The only shortcoming here is that we had to find not only the value of the Strouhal number, but we also had to allow  $k_f^{(fit)}$  to deviate (slightly) from the actual value of  $k_f$ . Although the difference between the two is perhaps not unreasonable, one would like to have some theoretical understanding of this discrepancy.

It is remarkable that in all three experiments the value of the Strouhal number depends only weakly on  $k_f$ . This suggests that the relaxation time  $\tau$  decreases with increasing values of  $k_f$ ; see Eq. (13). We also emphasize that St is similar in all three experiments, even though the wavenumber corresponding to the variation of the mean concentration changed significantly. This suggests that  $\tau$  does not depend on the scale of the concentration, even though such a dependence is in principle being allowed for [25, 27].

The method used in the present paper to determine the Strouhal number from simulations can straightforwardly be applied to magnetohydrodynamics. In that case the magnetic field plays the role of the passive scalar gradient. Both satisfy very similar equations and in both cases a mean field can easily be applied while still retaining fully periodic boundary conditions. In both cases the closure approach of Blackman and Field predicts non-Fickian turbulent diffusion and hence the occurrence of an extra time derivative [14, 15]. Another application would be to determine the role of an extra time derivative in connection with turbulent viscosity. In that case a mean gradient could be imposed using the shearing box approximation [35, 36]. The first two methods described

in the present paper should also still be applicable in that case. An obvious question that arises in this connection is whether non-Fickian diffusive properties could also play a role in attempts to find useful subgrid scale models for Large Eddy Simulations. The difficulty here is that one has to deal with averages that do not satisfy the Reynolds rules. Apart from this difficulty there should be no reason why an extra time derivative should not also be incorporated in such simulations.

## Acknowledgments

We thank Eric Blackman and Günther Rüdiger for interesting comments on our paper. P.K. acknowledges the financial support from the Magnus Ehrnrooth foundation and the travel support from DFG Graduate School ‘Non-linear Differential Equations: Modelling, Theory, Numerics, Visualisation. A.M. acknowledges the financial support from Hans Böckler Stiftung. P.K. and A.M. wish to thank Nordita and its staff for their hospitality during their visits. Use of the parallel computers in Odense (Horseshoe) and Leicester (Ukaff) is acknowledged.

---

[1] B. Eckhardt and J. Schumacher, Phys. Rev. **E 64**, 016314 (2001).

[2] T. Elperin, N. Kleeorin, I. Rogachevskii, and D. Sokoloff, Phys. Rev. **E 61**, 2617 (2000).

[3] H. K. Moffatt *Magnetic Field Generation in Electrically Conducting Fluids*. Cambridge University Press, Cambridge (1978).

[4] F. Krause and K.-H. Rädler *Mean-Field Magnetohydrodynamics and Dynamo Theory*. Pergamon Press, Oxford (1980).

[5] P. L. Sulem, Z. S. She, H. Scholl, and U. Frisch, J. Fluid Mech. **205**, 341 (1989).

[6] A. Brandenburg and B. v. Rekowski, Astron. Astrophys. **379**, 1153 (2001).

[7] G. Rüdiger *Differential rotation and stellar convection: Sun and solar-type stars*. Gordon & Breach, New York (1989).

[8] L. L. Kitchatinov and G. Rüdiger, Astron. Astrophys. **276**, 96 (1993).

[9] J.-P. Bouchaud and A. Georges, Phys. Rep. **195**, 127 (1990).

[10] R. B. Stull, J. Atmosph. Sci. **41**, 3351 (1984).

[11] R. B. Stull, Boundary Layer Meteorology **62**, 21 (1993).

[12] M. S. Miesch, A. Brandenburg, and E. G. Zweibel, Phys. Rev. **E61**, 457 (2000).

[13] A. Brandenburg and D. Sokoloff, Geophys. Astrophys. Fluid Dynam. **96**, 319 (2002).

[14] E. G. Blackman and G. B. Field, Phys. Rev. Lett. **89**, 265007 (2002).

[15] E. G. Blackman and G. B. Field, Phys. Fluids (2003). [astro-ph/0302013](http://arxiv.org/abs/astro-ph/0302013)

[16] A. K. Das, J. Appl. Phys. **70**, 1355 (1991).

[17] H.-T. Chen and K.-C. Liu, Comp. Phys. Comm., **150**, 31 (2003).

[18] N. Depireux and G. Lebon, J. Non-Newtonian Fluid Mech., **96**, 105 (2001).

[19] A. M. Weinberg and E. P. Wigner *The physical theory of neutron chain reactors*. University of Chicago Press, Chicago (1958), Chap. 9.

[20] W. W. R. Williams, Nucl. Sci. Eng. **135**, 123 (2000).

[21] H. T. Chen and J. Y. Lin, Int. J. Heat Mass Transfer **37**, 153 (1994).

[22] W. Israel, Phys. Rev. **153**, 1388 (1967).

[23] W. Kley and J. C. B. Papaloizou, Monthly Notices Roy. Astron. Soc. **285**, 239 (1997).

[24] M. K. Mak and T. Harko, Gen. Rel. Grav. **30**, 1171 (1998).

[25] S. A. Orszag, J. Fluid Mech. **41**, 363 (1970).

[26] M. Lesieur *Turbulence in Fluids*. Martinus Nijhoff Publishers (1990).

[27] K.-H. Rädler, N. Kleeorin, and I. Rogachevskii, Geophys. Astrophys. Fluid Dynam., in press (2003). [astro-ph/0209287](http://arxiv.org/abs/astro-ph/0209287)

[28] C. Cattaneo, On the conduction of heat, Atti Del Seminar. In: Modena 3, Mat. Fis. Univ. p. 3 (1948); see also M. P. Vernotte, Les paradoxes de la theorie continue de l'équation de la chaleur. Comptes Rendus Acad. Sci. 246, pp. 3154–3155 (1958).

[29] T. A. Yousef, A. Brandenburg, and G. Rüdiger, Astron. Astrophys. [astro-ph/0302425](http://arxiv.org/abs/astro-ph/0302425)

[30] A. Brandenburg, Astrophys. J. **550**, 824 (2001).

[31] We use the Pencil Code which is a cache efficient grid based high order code (sixth order in space and third order in time) for solving the compressible MHD equations; <http://www.nordita.dk/data/brandenb/pencil-code>.

[32] N. E. L. Haugen, A. Brandenburg, and W. Dobler, As-

trophys. J. Lett. [astro-ph/0303372](#)

[33] W. Dobler, N. E. L. Haugen, T. A. Yousef, and A. Brandenburg, Phys. Rev. **E**, in press (2003). [astro-ph/0303324](#)

[34] Animations can be found on <http://www.nordita.dk/~brandenb/movies/pscalar>.

[35] J. F. Hawley, C. F. Gammie, and S. A. Balbus, Astrophys. J. **440**, 742 (1995).

[36] A. Brandenburg, Å. Nordlund, R. F. Stein, and I. Torkelsson, Astrophys. J. **446**, 741 (1995).